Rheooptical Study on Poly(styrene macromonomer)

Tadashi Inoue,*,† Kenji Matsuno,† Hiroshi Watanabe,† and Yo Nakamura‡

Institute for Chemical Research, Kyoto University, Uji, Kyoto 611-0011, Japan, and Department of Polymer Chemistry, Graduate School of Engineering, Kyoto University, Katsura, Nishikyo-ku, Kyoto 615-8510, Japan

Received June 2, 2006; Revised Manuscript Received August 24, 2006

ABSTRACT: Dynamic birefringence and dynamic viscoelasticity of polymer brush type polystyrene polymacromonomer, PM, consisting of only styrene unit were measured over a wide frequency region including the glass transition region. The stress−birefringence relationship elucidated that the stress relaxation of the PM proceeded through three processes. The fastest one was attributed to the glassy component responsible for the high glassy modulus. This process was found to be essentially the same as that for the ordinary linear polystyrene, l-PS. The second one was assigned to be the reorientation process of the side chains. The viscoelastic segment size of the side chains was estimated to be about half of that for l-PS. This difference in size could be attributed to the reduction of nematic effect. The slowest one was assigned to the reorientation of the main chain. This process was described with the beads−spring theory with the viscoelastic segment about 3 times larger than that for l-PS. The large viscoelastic segment size of the main chain was fairly in accord with the large Kuhn segment size determined by light scattering experiments on the PM in dilute solution.

Introduction

Viscoelastic behavior and molecular dynamics of linear polymers have been investigated for long decades, and they are well-understood experimentally and theoretically. With the aid of the resent progresses of synthesis techniques, polymers having various well-defined chain architectures, such as hyperbranched polymers and dendric polymers, can be produced. These highly branched polymers would have hierarchical structures, and therefore the hierarchical stress relaxations are expected. Structural properties of these hyperbranched polymers have been studied with various scattering techniques. On the other hand, details of molecular dynamics responsible for the stress relaxation, particularly hierarchically natures of dynamics, remain to be discussed.

Polymerization of macromonomers is one of the methods to produce hyperbranched polymers. Controlling the molecular weight of macromonomer and polymerization condition, the ratio of the polymerization index of side chain, n_{side}, to main chain, n_{main}, can be varied. Depending on this ratio, $R = n_{side}/n_{main}$, polymacromonomers, PMs can be regarded as "molecular brushes" ($R \ll 1$, i.e., $n_{main} \gg n_{side} \gg 1$) or "hyperbranched (star) polymers" ($R \gg 1$).

PMs having molecular brush shape behave as semiflexible chains in solution.[1−3] Terao et al. studied chain dimension of PMs consisting only of polystyrene units in solution.[4−7] They showed that the contour length per main-chain residue is insensitive to the side-chain length, while the Kuhn segment length λ^{-1} (more generally, the stiffness parameter in the helical wormlike chain) under the Θ condition remarkably increases with increasing the side-chain length. Besides, those PMs form liquid crystalline phase in melt when the molecular weight of the side chains exceeds 3000.[8−10] The origin of this rigidity is attributed to the high segment density around the main chain.[11]

Dynamic properties of PMs in melt are rarely studied, particularly for the case of PMs consisting only of polystyrene units.[12−14] Vlassopoulos et al.[14] studied rheological properties of starlike PMs. In their study, n_{main} of the most samples is 10, and the largest n_{main} is 40, while n_{side} was relatively high. They found similarities in their soft ordering and dynamic response with other well-known model branched polymers such as multiarm stars, in that arm relaxation and structural rearrangements in a liquidlike order control their dynamics. For molecular brush type PMs, the effects of side chains on the interchain entanglements were investigated by rheological measurements, but details of the chain dynamics have not been clarified yet.[12,13]

The rheooptical method using birefringence measurements is a useful technique to study the reorientation dynamics of polymers. Kharchenko et al. applied the method to starlike polymers and found the breakdown of the stress−optical rule in the terminal flow region. They confirmed the existence of the additional relaxation in the terminal zone when branch density is high (∼50 arms).[15] They attributed the additional relaxation to the form birefringence of core−shell structure.

In the present study, we report the dynamic birefringence and dynamic viscoelasticity of a "molecular brush" type PM consisting only of polystyrene in a wide range of frequencies covering from the terminal flow zone to the glassy zone. The index, n_{side} of the PM is 15, which is far below the entanglement index, n_e, for linear PS in melt ($n_e = 170$). The index for main chain, n_{main}, is 745. If the side chain can be regarded as solvents, the effective concentration of repeating units constructing the main chain is estimated to be $1/n_{side} \sim 0.06$. At this concentration, n_e is expected to be larger than 2800 ($> n_{main}$) because n_e is inversely proportional to the concentration. Thus, our sample is free from the entanglement effect in both the side-chain and main-chain dynamics. Our interests are placed on the rheooptical response and molecular dynamics of semiflexible PMs. We will show that the rheooptical method is useful to distinguish the polymer dynamics involved in the hierarchical stress relaxation.

Experimental Section

Sample. α-Benzyl-ω-vinylbenzylpolystyrene, the styrene macromonomer,[5,6] was synthesized by living anionic polymerization in the manner reported by Tsukahara et al.[16,17] The product was

† Institute for Chemical Research.
‡ Department of Polymer Chemistry, Graduate School of Engineering.
* Corresponding author. E-mail: tinoue@scl.kyoto-u.ac.jp.

10.1021/ma061234r CCC: $33.50
Published on Web 10/05/2006

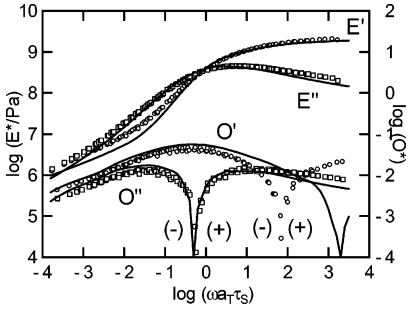

Figure 1. Composite curves for the complex strain−optical coefficient in tensile deformation and the complex Young's modulus for PM15. Error span is comparable to the mark size. Lines indicate the result for linear PS. The reference temperatures are 100 °C for PM15 ($\tau_s = 1.82$ ms) and 115 °C for l-PS ($\tau_s = 3.85$ ms).

reprecipitated five times from acetone solution into methanol to remove unreacted *p*-chloromethylstyrene. The molecular weight of the macromonomer was 1.65×10^3 when estimated from the weight-average molecular weight M_w of 1.53×10^3 of the precursor (α-benzyl-ω-vinylbenzylpolystyrene) determined by light scattering. The weight-average to number-average molecular weight ratio M_w/M_n for the precursor was estimated to be 1.09 by a MALDI-TOF spectrometer with a *trans*,*trans*-4,4-dephenyl-1,3-butadiene matrix containing silver ions in the form of $AgCF_3COO$; the value of M_w evaluated from the mass spectrum agreed with the light scattering value of 1.53×10^3 within 4%.

The macromonomer was polymerized in benzene at 45−60 °C for 50−100 h with azobis(isobutyronitrile) as an initiator to obtain the polymacromonomer samples. The product was purified and extensively fractionated from benzene/methanol mixtures. M_w of the PM was found to 1.23×10^6($n_{main} = 745$) and $M_w/M_n = 1.06$.

Rheooptical Measurements. The apparatus for rheooptical measurement was reported previously.[18,19] An optical system with a He−Ne laser, two polarizers, and a quarter wave plate was equipped with a vibron-type rheometer for the measurement of the oscillatory birefringence $\Delta n^*(\omega)$ under sinusoidal deformation at angular frequency, ω. The apparatus was used in both tensile and shear modes with tensile strain $\epsilon^*(\omega)$ or shear strain $\gamma^*(\omega)$. In the tensile mode,[18] the complex Young's modulus, $E^*(\omega)$, and strain−optical coefficient, $O^*(\omega) = \Delta n^*/\epsilon^*$, in tensile deformation were measured with strip specimens having 1 mm thickness (optical path length) in the temperature range 100−120 °C. In the shear mode,[19] the complex shear modulus, $G^*(\omega)$, and the complex strain−optical coefficient in shear, $K^*(\omega)$, defined as $\Delta n^*/2\gamma^*$, were determined with a shear fixture having 5 mm optical path length in the temperature range from 120 to 150 °C. To check the compliance correction in shear mode, $G^*(\omega)$ was measured with a Rheometric ARES system.

Results and Discussion

The Glass Transition Zone. Figure 1 shows $E^*(\omega)$ and $O^*(\omega)$ for PM15 around the glass transition region. Here, we used the method of reduced variables to construct the composite curves.[20] Dotted lines in the figure represent results for the linear polystyrene, l-PS, having $M_w = 2.5 \times 10^5$. To take into account the difference of the glass transition temperature between two polymers, the frequencies are reduced by $\tau_s = 1/\omega_C$. Here, ω_C is the crossing frequency at which $E' = E''$ in the glassy zone. The temperature dependence of the shift factors for E^* and O^*, a_T, for PM15 is not shown here, but it is essentially the same as that for linear polystyrene if the difference of the glass transition temperature was considered.

E^* for PM15 and l-PS are quite similar to each other. However, one important difference is that E' of PM15 is higher than l-PS in the transition zone ($-4 < \log(\omega/s^{-1}) < -1$). On the other hand, O^* of the two polymers are approximately the same at low frequencies in contrast to the above-mentioned difference in E'. The difference in O^* is observed at high frequencies: O' for PM15 changes its sign at a frequency lower than that for l-PS. O'' for PM is slightly higher than that for l-PS in the glassy zone. According to the modified stress−optical rule, MSOR,[18] which describes the relationship between the stress and birefringence around the glass transition zone, the positive birefringence for PS can be attributed to the glassy component, as will be described later. Therefore, the change of sign at the lower frequency means that the glassy component of O^* for PM is more significant than that for l-PS. This is the main reason why O' for PM changes its sign at a low frequency.

For the case of linear polymers in melt, the stress−optical rule holds well between the strain-induced birefringence and stress.[21] The rule is written for oscillatory tensile deformations with small amplitude.

$$E^* = C_R O^* \tag{1}$$

The proportionality coefficient, C_R, referred to as the stress−optical coefficient, can be related with the anisotropy of polarizability of the segments, $\Delta\beta$.[22] For the case of PM15, the ratio of O' to E' becomes constant at low frequencies, and therefore we estimated $C_R \equiv O'/E'$ as 2.7×10^9 Pa^{-1}. This value is smaller than that for linear polystyrenes (4.8×10^9 Pa^{-1}).

MSOR Analysis. The SOR does not hold well in the glass-to-rubber transition zone. Alternatively, the MSOR holds well for various linear polymers.[18] For the case of PM, the molecular dynamics may be much more complex than those for liner polymers. However, it would be worthwhile to examine the ordinary MSOR considering two relaxation processes. The MSOR for tensile deformations is written as follows:

$$E^*(\omega) = E_R^*(\omega) + E_G^*(\omega) \tag{2}$$

$$O^* = C_R E_R^*(\omega) + C_G E_G^*(\omega) \tag{3}$$

The two proportional coefficients, C_R and C_G, could be respectively determined from the proportionality between O' and E' in the transition zone and the proportionality between O'' and E'' in the glassy zone. The obtained C_R and C_G values are summarized in Table 1.

Table 1. Stress−Optical Coefficients and Characteristic Parameters for PM15 and l-PS

code	$10^{-7}E_R'(\infty)$/ Pa	$10^9 C_R$/ Pa^{-1}	$10^{11} C_G$/ Pa^{-1}	$10^1 \Delta n_0$	M_S/ g mol^{-1}
PM15	2.1	−2.7	3.6	−0.89	450
l-PS	1.2	−4.8	3.0	−1.0	850

For these C_R and C_G values, the simultaneous equations (2) and (3) for E_R^* and E_G^* were solved at each temperature. The obtained E_R^* and E_G^* are shown in Figure 2. Here, we used the method of reduced variables separately to construct the composite curve for each component.[20] For comparison, the result for l-PS is also included in the figure.

The separation of E^* into E_R^* and E_G^* seems to be reasonable for PM15 as well as the ordinary linear polymers. The G component is almost the same for PM15 and l-PS, indicating the G component is insensitive to the chain branching. The local dynamics responsible for the G component would not be affected by details of chain architecture. This may be natural because the molar ratio of the branching point to the total monomer is not so high: Since n_{side} for PM15 is 15, the relative concentration of monomers at branching point is about $1/n_{side} = 6.7$ mol %, and therefore E_G^* mainly reflects the dynamics of linear part of the side chains.

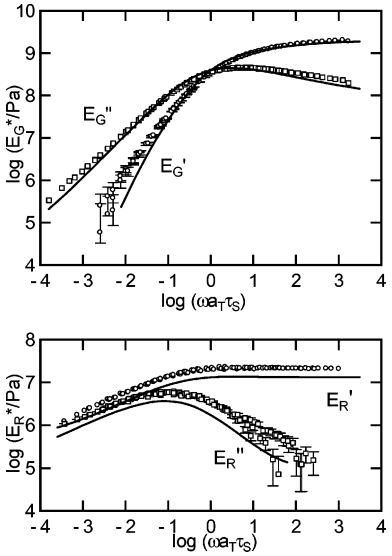

Figure 2. Results of MSOR analysis for PM15. Error bars indicate the uncertainty span due to error of the estimation of the two stress−optical coefficients. Lines indicate the results for linear PS. The reference temperatures are the same as Figure 1.

On the other hand, the R component, E_R*, for PM15 is about 2 times larger than that for l-PS over the whole frequency range studied. This result is consistent with that E' for PM15 is higher than that for l-PS in the transition zone, as noted in Figure 1. We note that the relative concentration of monomers consisting of main chain is only 6.7%, and therefore E_R* mainly reflects the dynamics of the linear part of the side chains.

The limiting modulus of E_R' at high frequencies, $E_R'(\infty)$ ($\equiv 3G_R'(\infty)$), may be related to the molecular weight of the viscoelastic segment, M_S.

$$M_S = \frac{\rho RT}{G_R'(\infty)} \tag{4}$$

Here, ρ, R, and T are the density, gas constant, and temperature, respectively. M_S may be related with the Kuhn segment size, M_K, with the following equation:[23]

$$\frac{M_S}{M_0} = c_1 \frac{\Delta\beta}{\Delta\alpha} = c_1 c_2 c_3 \frac{M_K}{M_0} \tag{5}$$

Here, $\Delta\alpha$ and M_0 are respectively the optical anisotropy and the molecular weight of the repeating unit. The ratio $\Delta\beta/\Delta\alpha$ represents the optical segment size. The parameters c_1, c_2, and c_3 are respectively determined by the effect of nonaffine deformation, the strength of the nematic interaction,[24] and the chain statistics. $c_1 = 1$ corresponds to the affine-like orientation of the chain axis of repeating units. For the case of polymer melts, the value of c_1 can be regarded as unity although c_1 could become considerably large in dilute solutions, $c_1 \sim 5$. From the rheooptical studies on polymer blends, the nematic interaction parameter, δ, is estimated to be about 0.3, [25−27] which results in $c_2 = 1/(1 - \delta) \sim 1.3$. The c_3 parameter characterizes the ratio of the optical segment size to the Kuhn segment size, $(\Delta\beta/\Delta\alpha)/(M_K/M_0)$, when the nematic interaction can be ignored ($c_2 = 1$), and its value is expected to be about 0.8 for polymers having the tetrahedral bond angle like PS.[23,28] As a result, the M_S value is apparently very close to the M_K value.[29]

The obtained value of M_S for PM15 is about 400 g mol^{-1}, which is about half of M_S for l-PS. In the following, we consider the molecular origin of the anomalously smaller M_S for PM15. First of all, we note that C_R for PM15, a parameter reflecting the optical segment size, $\Delta\beta$, is about half of C_R for l-PS, and that this result is in accord with the reduction of M_S. (Note that the value of C_R was directly determined from the comparison of E* and O* data, and therefore it is free from uncertainty arising from the MSOR analysis.) As a result, $O_R'(\infty) = C_R E_R'(\infty)$, reflecting the initial orientation in the glassy zone, is almost the same between PM15 and l-PS. This means that $\Delta\beta/M_S \sim C_R E_R'(\infty)$ is almost the same, and therefore the c_1 value for PM15 is also unity as c_1 for l-PS is. Thus, the orientation caused by the deformation is very similar in the monomeric level between the two polymers. In other words, the monomers composing the side chains orient so that the chain axis of the side chain orients to the stretch direction similarly to that of the repeating units in the linear PS do. In addition, $c_1 \sim 1$ corresponding to the initial orientation may be described with the pseudo-affine orientation.[30] This would be natural because the chain contour of the side chain would be deformed affinely in the glassy zone. If the contour is not deformed affinely, the local strain becomes inhomogeneous, and the viscoelastic properties of the PM would be much different from those for linear chains.

The smaller C_R and M_S values for PM can be obtained by smaller c_2, c_3, and M_K values. The smaller M_K value means the change of the statistics of side chain. It is widely accepted that the rotational hindrance for main chain carbon−carbon bonds strongly affects the chain statistics. High segment density due to branching may reduce the effective magnitude of the rotational hindrance. Such an effect can reduce the M_K value of the side chains. The change of the statistics of side chain also affects the c_3 parameter in eq 5,[31] and therefore the smaller M_S value may be originated from the change of c_3. However, this would be a minor effect because c_3 is sensitive to the bond angle but not to the rotational hindrance.[28] Here we briefly summarized the studies on the chain conformation of the side chain of polymer brushes. Schmidt et al. suggested from the small-angle X-ray scattering experiments on their *s*-PS-*b*-PAMA that the side chain would have an extended chain conformation,[1] and some computer simulations[32−34] support the extended conformation. However, Nakamura and co-workers[4−7] concluded from the experimental results that the side chains adopt the same conformation as a free, linear chain, as did Gauger and Pakula[35] and Siokawa, Itoh, and Nemoto.[36] Thus, we may conclude that the change of chain statistic for the side chain would be quite small. Therefore, we note another possible origin for the smaller C_R and M_S values. As shown in a previous paper, the nematic effect increases the c_2 parameter[37] (see eq 5). The nematic effect may be reduced for the polymacromonomers due to the branched architecture. The M_S value for polystyrenes without the nematic interaction may be expected to be approximately $c_3 M_S \sim 600$.[23,25] This value suggests that the reduction of the nematic effect might contribute to the smaller M_S value for PM15.

Terminal Flow Region. Figure 3 shows G* and K* for PM15 from the transition zone to the flow region. Here, we used the method of reduced variables to construct the composite curve.[20] Also included are G* data obtained by the conventional rheometer to check the consistency of data. We tried to extend the measurements of G* and K* at higher temperature, but the reliable data were not obtained because of the sample flow.

In Figure 3, G' and G'' roughly obey a power law relationship, $G' \sim G'' \sim \omega^{1/2}$, at low frequencies. However, a careful observation reveals that G' relaxes in two steps. This result is

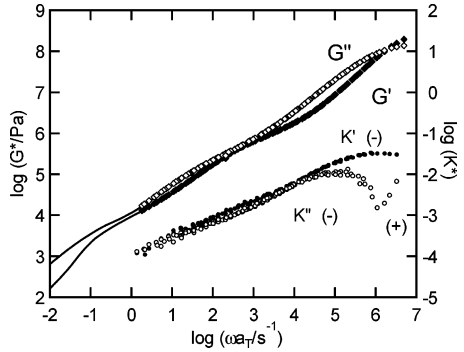

Figure 3. Complex strain−optical coefficient in shear, K^*, and the complex modulus, G^*, for PM15. Error span is comparable to the mark size. The reference temperature is 140 °C.

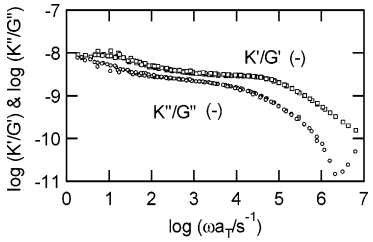

Figure 4. Frequency dependence of the ratio of K'/G' and K''/G''. Error span is comparable to the mark size.

consistent with the results for *s*-PS-*b*-PMA polymacromonomers.[13]

Figure 4 displays the K'/G' and K''/G'' ratio at low frequencies. K'/G' shows two plateaus. The plateau value at high frequencies agrees with C_R estimated by the tensile measurement. On the other hand, the value of K'/G' at low frequencies ($\log(\omega/s^{-1}) < 1$) is about 3 times larger than that at high frequencies. These results indicate that two relaxation mechanisms are involved in G^* or K^* at these frequencies, and the stress−optical rule holds valid for each component.

Separation of Relaxation Modes. Considering the above results, we assume that G^* and K^* include three components of dynamics. For such a case, G^* and K^* may be written as follows:

$$G^* = G_T^* + G_B^* + G_G^* \tag{6}$$

$$K^* = C_T G_T^* + C_B G_B^* + C_G G_G^* \tag{7}$$

Here, subscripts represent trunk, branch, and glass. The two stress−optical coefficients, C_T and C_B, can be determined from Figure 4. To solve these simultaneous equations, we need further assumptions. We assume that G_G^* can be estimated by extrapolating the E_G^* ($=3G_G^*$) data shown in Figure 2 to low frequencies. Thus, eqs 6 and 7 are reduced to

$$G^* - G_G^* = G_T^* + G_B^* \tag{8}$$

$$K^* - C_G G_G^* = C_T G_T^* + C_B G_B^* \tag{9}$$

These simultaneous equations can be solved for G_T^* and G_B^*. The obtained G_T^* and G_B^* are shown in Figure 5.

As described before, G_G^* of PM supports the high glassy modulus and is quite similar to that of the ordinary linear polystyrene. Thus, G_G^* is insensitive to chain architecture. On the other hand, G_B^* located between G_G^* and G_T^* would reflect the reorientational motion of the side chains. The frequency dependence of $G_B^* \sim \omega^{1/2}$ is very similar to the prediction of the Rouse model. Characteristic features of G_G^* and G_B^* were

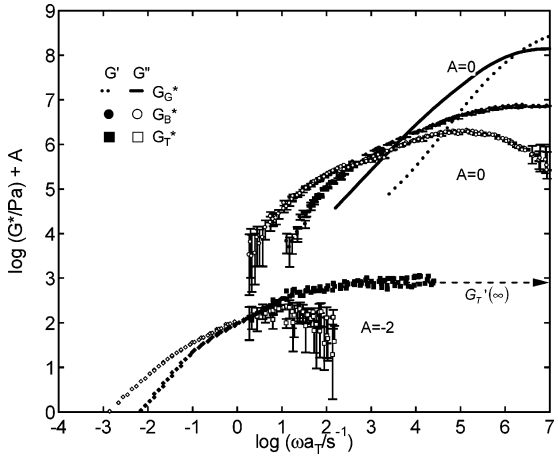

Figure 5. Separation of modulus into three components representing glass, trunk, and branch relaxation. The reference temperature is 140 °C.

respectively discussed as E_G^* and E_R^* in the previous section, and therefore we do not repeat them here.

The slowest component, G_T^*, becomes dominant in the low frequencies and would reflect the reorientation of the main-chain backbone. Although n_{main} is larger than n_e, the entanglement effect, which can be recognized as a rubbery plateau region, is not observed for main-chain relaxation, G_T^*, as we expected. The effective concentration of the main chain is too low to entangle. The frequency dependence of G_T^* is also very similar to that of the Rouse model. This means that dynamics of the brush-type polymers can be described with a linear chain with a coarse-graining structure unit. Such a unit is conceptually similar to a "superblob", which has been used for the calculation of scattering form factor for branched polymers.[38−40]

The value of the limiting modulus for G_T^* at high frequencies, $G_T'(\infty)$, was estimated to be 8.9×10^4 Pa. The viscoelastic segment size of main-chain backbone, M_S^T, is estimated to be 3.9×10^4 g mol^{-1} by analogy with eq 4.

$$M_S^T = \frac{\rho RT}{G_T'(\infty)} \tag{10}$$

The M_S^T value is fairly in accord with the Kuhn segment size of PM15 in cyclohexane, M_K^T, being estimated by light scattering experiments to be 6.0×10^4 g mol^{-1}.[5] From the M_S^T value, we can estimate the number of macromonomers per viscoelastic segment for main chain as $3.9 \times 10^4/1.65 \times 10^3 \sim 24$. This value is ~3 times larger than that for linear PS, indicating that the main chain of PM15 is about 3 times less flexible than the linear polystyrene.[41]

For the case of linear chains in melt, the viscoelatic segment size can be related to the Kuhn segment size with eq 5.[23] We expect that the similar relation would hold between M_S^T and M_K^T for PM systems. Slightly smaller M_S^T than M_K^T may be related to a different c_3 value. The c_3 value for main chain might be different from that for liner polymers. Calculation of c_3 value for branched chains is desired. The nematic interaction between main chains may be reduced because the side chains would decrease the direct contact between main chains. Such an effect of side chains might give the smaller M_S^T value through the reduction of the nematic effect. Here, we should note that PMs having higher n_{side} behave as nematic liquid crystalline polymers. In this context, the nematic interaction becomes significant for PMs with high n_{side} values. Thus, the role of the nematic interaction in PM systems is not clear, and further studies are desired.

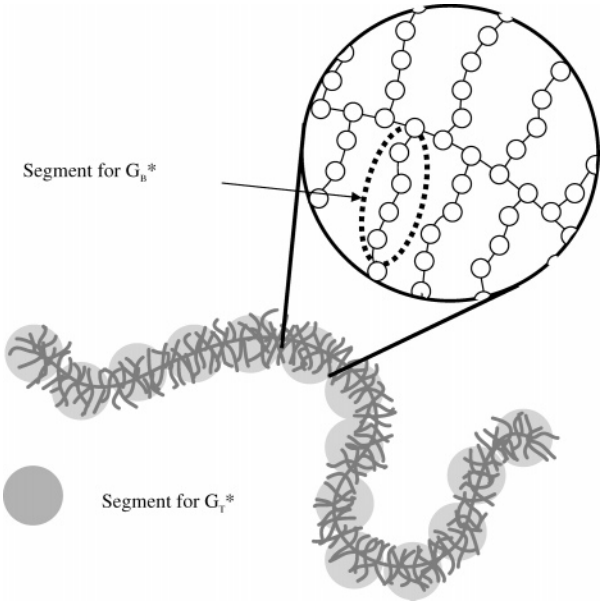

Figure 6. Schematic illustration of viscoelastic segments for G_B^* and G_T^* components.

The good correspondence between the viscoelastic and Kuhn segments of main chain ($M_K^T/M_S^T < 1.6$) supports our assignment that G_T^* reflects the reorientational motion of main chain induced by the shear flow. In addition, we emphasize the result of $G_T^* \sim \omega^{1/2}$, which means that dynamics of the main chain can be described with the bead−spring model for linear chains. In other words, dynamics of the brush-type polymers in the flow region can be regarded as a linear chain by an adequate coarse-graining operation.

In connection with dynamics of the main chain, we should note C_T is negative. As described before, Kharchenko et al. applied the rheooptical method to hyperbranded polymers and showed the breakdown of the stress−optical rule in the terminal region.[15] They found the existence of the additional relaxation associated with the positive form birefringence of core−shell type structure. Since the form birefringence is always positive, the negative value of C_T for PM15 cannot be attributed to the form birefringence of PM.

On the analogy of the molecular theory for the strain-induced birefringence for linear chain, C_T would be related to the anisotropy of the backbone segment. As noted before, the main chain of PM15 is about 3 times less flexible than l-PS. In this context, we expect that C_T would be about 3 times larger than C_R for l-PS. This prediction, -1.4×10^{-8} Pa^{-1}, is fairly close to the measured value of C_T, -9.5×10^{-9} Pa^{-1}. The measured value of C_T, which is twice of C_R for l-PS, corresponds to anisotropy of ∼16 styrene units since C_R for l-PS corresponds to anisotropy of 8 styrene units. Note that the viscoelastic segment of the main chain is composed of approximately $3.9 \times 10^4/104 \sim 380$ styrene units. Thus, the C_T value indicates that the orientation of side chains would have relaxed at low frequencies, and more importantly they would have no particularly orientated conformations in the scales of the viscoelastic segments of the main chain.

Figure 6 displays a schematic illustration of G_B^* and G_T^* components deduced from the above analysis. By the coarse graining of the chain, PM may be regarded as an ordinary linear chain but with the larger segment size. As described before, the number of the segment per main chain is ∼24. The dynamics of the main-chain segments is very similar to the Rouse model.

The reorientational dynamics of the side chain may be affected by the branched chain architecture. The experimentally determined viscoelastic segment size of the side chain was about half of the segment size for the ordinary linear PS. On the other hand, the fast local dynamics over a few repeating units, related to the glass transition, may not be affected by the branching: Although the local dynamics of the repeating units around the branching point may be affected by the branching, the concentration of such units is small for polymers having long side chains. From this reason, the glassy component of the PM agrees with that of the linear PS, as noted experimentally.

In the present experiments, we did not see the effect of entanglements on both dynamics of the side chain and main chain as described before. With increasing n_{side} or n_{main}, we will see the effect of entanglements on both the reorientation processes. For such relaxation processes, it is an interesting issue whether the sophisticated tube theories such as tube dilation theory can be applicable or not. Also of interest is to see how the difference in viscoelastic segment length between the main and side chains affects the entanglement dynamics. The possibility of such experiments is now under consideration.

The present measurements were performed on only one bottle brush-type polymacromonomer. In general, the viscoelastic stress of branched polymers would relax hierarchically corresponding to the hierarchical nature of the structure. We expect that the rheooptical separation of stress would work well for other branched polymers. The measurements on other types of branched polymers will be reported in the future.

Concluding Remarks

We examined dynamic birefringence and dynamic viscoelasticity for a model polymacromonomer having brush-type chain architecture over a wide frequency region including the glass transition region. Since the polymacromonomer was composed of only styrene, the segregation effect between different monomers could be ignored. We showed that the stress relaxation process of this model polymacromonomer could be separated into three processes, the glassy, branch, and trunk modes, being characterized with different stress−optical coefficients.

The fastest glassy process was very similar to that for the ordinary linear polystyrene except for reducing the glass transition temperature, which can be attributed to the high number density of chain ends having large free volume. The similarity of the glassy process may be natural because the number of branching monomer is less than 7 mol %.

The second relaxation process was assigned to be the reorientation process of the side chain. The stress−optical coefficient of this process was found to be negative. This means that the chain contour of the side chain orients along the stretching direction. This could be possible if the chain contour of side chain deformed affinely. The estimated viscoelastic segment size of side chain was about half of that for l-PS, which means each side chain composed of about four styrene units. The smaller segment size could be related to the high segment density in PM through the change of chain statistics or more possibly the reduction of the nematic effect between the segments. In general, the segments size along the side chain may vary depending on the distance from the main-chain backbone. However, in the present study, the relaxation process of the side chain was well described with a single stress−optical coefficient, which strongly suggests the uniformity of the segment size of the side chain.

The slowest process was assigned to the reorientation of the main-chain backbone. The effect of entanglement was not

observed because the effective main-chain concentration was low. The distribution of the relaxation times of this process was described with the bead−spring theory. The dynamics of the brush-type polymers can be described with a linear chain with a coarse-graining structure unit, conceptually similar to the superblob used for the calculation of scattering form factor for branched polymers. The estimated viscoelastic segment size was about 3 times larger than that for l-PS. This large segment size of PM was fairly in accord with the Kuhn segment size determined from independent light scattering experiments. The present study indicates that hierarchical dynamics of branched polymers can be separated by the rheooptical method.

Acknowledgment. This study was partially supported by a Grant-in-Aid for Scientific Research (No. 17540381) from the Ministry of Education, Culture, Sports, Science, and Technology of Japan.

References and Notes

(1) Wintermantel, M.; Gerle, M.; Fischer, K.; Schmidt, M.; Wataoka, I.; Urakawa, H.; Kajiwara, K.; Tsukahara, Y. *Macromolecules* **1996**, *29*, 978−983.
(2) Nemoto, N.; Nagai, M.; Koike, A.; Okada, S. *Macromolecules* **1995**, *28*, 3854−3859.
(3) Wintermantel, M.; Schmidt, M.; Tsukahara, Y.; Kajiwara, K.; Kohjiya, S. *Macromol. Rapid Commun.* **1994**, *15*, 279−284.
(4) Terao, K.; Takeo, Y.; Tazaki, M.; Nakamura, Y.; Norisuye, T. *Polym. J.* **1999**, *31*, 193−198.
(5) Terao, K.; Nakamura, Y.; Norisuye, T. *Macromolecules* **1999**, *32*, 2, 711−716.
(6) Terao, K.; Hokajo, T.; Nakamura, Y.; Norisuye, T. *Macromolecules* **1999**, *32*, 3690−3694.
(7) Hokajo, T.; Terao, K.; Nakamura, Y.; Norisuye, T. *Polym. J.* **2001**, *33*, 481−485.
(8) Maeno, K.; Nakamura, Y.; Terao, K.; Sato, T.; Norisuye, T. *Kobunshi Ronbunshu* **1999**, *56*, 254−259.
(9) Tsukahara, Y.; Ohta, Y.; Senoo, K. *Polymer* **1995**, *36*, 3413−3416.
(10) Wintermantel, M.; Fischer, K.; Gerle, M.; Ries, R.; Schmidt, M.; Kajiwara, K.; Urakawa, H.; Wataoka, I. *Angew. Chem., Int. Ed. Engl.* **1995**, *34*, 1472−1474.
(11) Nakamura, Y.; Norisuye, T. *Polym. J.* **2001**, *33*, 874−878.
(12) Namba, S.; Tsukahara, Y.; Kaeriyama, K.; Okamoto, K.; Takahashi, M. *Polymer* **2000**, *41*, 5165−5171.
(13) Tsukahara, Y.; Namba, S.; Iwasa, J.; Nakano, Y.; Kaeriyama, K.; Takahashi, M. *Macromolecules* **2001**, *34*, 2624−2629.
(14) Vlassopoulos, D.; Fytas, G.; Loppinet, B.; Isel, F.; Lutz, P.; Benoit, H. *Macromolecules* **2000**, *33*, 5960−5969.
(15) Kharchenko, S. B.; Kannan, R. M. *Macromolecules* **2003**, *36*, 407−415.
(16) Tsukahara, Y. *Macromolecular Design: Concept and Practice*; Mishra, M. K., Ed.; Polymer Frontiers International: New York, 1994; pp 161−227.
(17) Tsukahara, Y.; Inoue, J.; Ohta, Y.; Kohjiya, S.; Okamoto, Y. *Polym. J.* **1994**, *26*, 1013−1018.
(18) Inoue, T.; Okamoto, H.; Osaki, K. *Macromolecules* **1991**, *24*, 5670−5675.
(19) Onogi, T.; Inoue, T.; Osaki, K. *Nihon Reoroji Gakkaishi* **1998**, *26*, 237−241.
(20) Ferry, J. D. *Viscoelastic Properties of Polymers*, 3rd ed.; Wiley: New York, 1980.
(21) Janeschitz-Kriegl, H. *Polymer Melt Rheology and Flow Birefringence*; Springer-Verlag: Berlin, 1983.
(22) Kuhn, W.; Grun, F. *Kolloid Z.* **1942**, *101*, 248.
(23) Inoue, T. *Macromolecules* **2006**, *39*, 4615−4618.
(24) Tanaka, T.; Allen, G. *Macromolecules* **1974**, *10*, 426−430.
(25) Messe, L.; Prud'homme, R. E. *J. Polym. Sci., Polym. Phys. Ed.* **2000**, *38*, 1405−1415.
(26) Ylitalo, C. M.; Kornfield, J. A.; Fuller, G. G.; Pearson, D. S. *Macromolecules* **1991**, *24*, 749−758.
(27) Ylitalo, C. M.; Zawada, J. A.; Fuller, G. G.; Abetz, V.; Stadler, R. *Polymer* **1992**, *33*, 2949−2960.
(28) Volkenstein, M. V. *Configurational Statistics of Polymeric Chains*; Interscience: New York, 1963.
(29) Inoue, T.; Osaki, K. *Macromolecules* **1996**, *29*, 1595−1599.
(30) Kratky, O. *Kolloid-Z.* **1933**, *64*, 213.
(31) Flory, P. J. *Statistical Mechanics of Chain Molecules*; John Wiley & Sons: New York, 1969.
(32) Murat, M.; Grest, G. *Macromolecules* **1991**, *24*, 704−708.
(33) Rouault, Y.; Borisov, O. V. *Macromolecules* **1996**, *29*, 2605−2611.
(34) Saariaho, S.; Szleifer, I.; Ikkala, O.; ten Brinke, G. *Macromol. Theory Simul.* **1998**, *7*, 259.
(35) Gauger, A.; Pakula, T. *Macromolecules* **1995**, *28*, 190−196.
(36) Shiokawa, K.; Itoh, K.; Nemoto, N. *J. Chem. Phys.* **1999**, *111*, 8165−8173.
(37) Oh, G. K.; Inoue, T. *Rheol. Acta* **2005**, *45*, 116.
(38) Birshtein, T.; Borisov, O.; Zhulina, E.; Khokhlov, A.; Yurasova, T. *Polym. Sci. U.S.S.R.* **1987**, *29*, 1293.
(39) Halperin, A.; Tirrell, M.; Lodge, T. P. *Tethered Chains in Polymer Microstructures*; 1992; Vol. 100, p 31.
(40) Rathgeber, S.; Pakula, T.; Wilk, A.; Matyjaszewski, K.; Beers, K. L. *J. Chem. Phys.* **2005**, *122*.
(41) With the similar argument on slightly larger Kuhn segment of 6.0×10^4, we may say that PM15 is about 5 times less flexible than the linear PS from the geometrical aspect. The difference arises from the difference in M_T and M_K.

MA061234R